Annals of Biomedical Engineering, Vol. 47, No. 4, April 2019 (© 2019) pp. 1094–1105
https://doi.org/10.1007/s10439-019-02200-9

A Mechanistic Analysis of Possible Blood Transfusion Failure to Increase Circulatory Oxygen Delivery in Anemic Patients

ROBERT A. ZIMMERMAN,[1] AMY G. TSAI,[2] MARCOS INTAGLIETTA,[2] and DANIEL M. TARTAKOVSKY[3]

[1]Los Alamos National Laboratory, Los Alamos, NM 87545, USA; [2]Department of Bioengineering, University of California, San Diego, 9500 Gilman Drive, La Jolla, CA 92093, USA; and [3]Department of Energy Resources Engineering, Stanford University, 367 Panama Street, Stanford, CA 94305, USA

(*Received 11 October 2018; accepted 5 January 2019; published online 18 January 2019*)

Associate Editor Umberto Morbiducci oversaw the review of this article.

Abstract—The effects of changing hematocrit (Hct) on the rate of circulatory oxygen (O_2) delivery were modeled analytically to describe transfusion of 0.5–3.0 units of packed red blood cells (pRBC, 300 mL/unit, 60% Hct) to anemic patients. In our model, Hct affects O_2 delivery to the microcirculation by changing blood O_2 carrying capacity and blood viscosity, which in turn affects blood flow velocity and, therefore, O_2 delivery. Changing blood velocity impacts the O_2 delivery by affecting the oxygen diffusive losses as blood transits through the arteriolar vasculature. An increase in Hct has two opposite effects: it increases the blood O_2 carrying capacity and decreases the flow velocity. This suggests the existence of an optimal Hct that maximizes O_2 delivery. Our results show that maximal O_2 delivery occurs in the anemic range, where Hct < 39%. Optimal blood management is associated with transfusing enough units up to reaching maximal O_2 delivery. Although somewhat complex to implement, this practice would result in both substantial blood savings and improved O_2 delivery.

Keywords—Oxygen delivery, Oxygen carrying capacity, Blood transfusion.

INTRODUCTION

When used to treat blood loss due to trauma or surgical interventions, blood transfusion restores blood volume, systemic pressure, and oxygen delivery (D_{O_2}). Blood transfusion is also deployed to treat anemia by transfusing packed red blood cells (RBCs) at a high hematocrit (Hct), so that blood oxygen carrying capacity (Ca_{O_2}) increases but blood volume is minimally affected.

Address correspondence to Daniel M. Tartakovsky, Department of Energy Resources Engineering, Stanford University, 367 Panama Street, Stanford, CA 94305, USA. Electronic mail: tartakovsky@stanford.edu

Anemia, defined by Hct < 33–39%, is typically treated by transfusing 1–3 units of blood,[25] a practice that uses up to 1/3 of the total blood supply. Anemia-related negative events tend to increase when patients are transfused at lower Hct or hemoglobin (Hb) levels. However, some patient groups do not show improvements upon transfusion to higher Hb thresholds.[8]

Many studies in humans and canines report that maximal D_{O_2} occurs at an optimal Hct that is somewhat lower than normal. Crowell *et al.*[9] were among the first to note the dual role and opposing effects of increasing Hct in order to enhance Ca_{O_2}: by increasing the blood viscosity it reduces the blood flow and D_{O_2}. Carried out in dogs, such experiments (see also Refs. 10, 41) revealed that maximal D_{O_2} occurs at Hct $\approx$ 42%. Optimal Hct was also found to be organ-dependent, e.g., being 48.7% for canine intestine.[43] Studies in humans show similar results, although optimal Hct is reported to be somewhat lower than in canines, in the range of 30–33%, and organ-dependent as well, e.g., it is 35.2% in the human brain.[22]

Blood flow velocity is an additional factor regulating D_{O_2} to the nutrient microcirculation, independently of its role in setting the rate of RBC delivery. This is due to the diffusive losses of O_2 from blood vessels. These are driven by the large O_2 gradient between systemic arterial blood and the surrounding tissue, because a blood vessel wall is not a barrier to O_2 diffusion. The diffusion coefficient for O_2 in the blood vessel wall is similar to that of other tissues.[26]

Consequently, a quantitative assessment of the effects of changing Hct on D_{O_2} should account for variability in flow velocity, transit time of blood in the circulation, and the amount of O_2 that diffuses out at each vascular segment. The loss of O_2 from

0090-6964/19/0400-1094/0 © 2019 Biomedical Engineering Society

microvessels increases as blood flow velocity decreases and, hence, the O_2 residence time in the vessels increases. The O_2 loss from arterial vessels was first highlighted in Ref. 12, wherein significant longitudinal O_2 gradients in arteriolar vessels were also observed. This phenomenon was analyzed in Ref. 35, leading to the conclusion that "retardation of blood flow may cause a significant increase in precapillary O_2 losses". Subsequent modeling studies[22,30] demonstrated the critical role of blood viscosity in determining D_{O_2}. Several analytical and numerical investigations[26,35,37] quantified the O_2 losses in arterial blood vessels, without explaining how changes in Hct affect D_{O_2}. Comparison of the observed O_2 losses from arterioles with those predicted by the simplified analytical models of O_2 diffusion into the parenchymal tissue revealed that the latter underestimates the former.[37,54]

Advection-diffusion-reaction transport of O_2 in a three-dimensional capillary network was analyzed in Refs. [5,6] by using a model comprising coupled nonlinear elliptic differential equations, which were solved numerically using a finite-difference method. The model relates an increase in myoglobin concentration to an increase the O_2 consumption rate in the surrounding tissue, which results in alleviating hypoxia. While this model accounts for Hct, it does not explicitly explore the impact of changes in Hct on O_2 consumption.

Most studies agree that the diffusive losses of O_2 occur over the entire network. However, small residence times of O_2 in the larger vessels render these losses negligible in larger vessels. We therefore posit that the effects of changes in Hct on the O_2 delivery in the microcirculation can be adequately captured by a mechanistic model of a single arteriole. We suggest that the losses observed in a single arteriole (evaluated in vessels throughout the arteriolar network) are representative of the magnitude of D_{O_2} changes in response to changes in Hct. Our analysis aims to predict three quantities of interest with a fully analytical model of O_2 transport in an arteriole vessel: (i) the dependence of D_{O_2} on Hct, (ii) the impact of each unit of pRBCs transfused to an anemic patient, and (iii) the amount of O_2 lost through the vessel walls over the length of each arteriole.

In "Materials and Methods" section, we present an analytical model of O_2 transport in an arteriole. Physiologically relevant parameters and corresponding model predictions of the dependence of D_{O_2} on Hct are presented in "Results" section. Main conclusions and their implications for blood transfusion are discussed in "Discussion" section.

MATERIALS AND METHODS

Physiological Considerations

Whole blood consists of RBCs, platelets and leukocytes suspended in plasma. Yet, it is common to treat blood as a homogeneous continuum fluid as long as flow takes place in blood vessels whose diameter is larger than 15 μm (Refs. 19, 45 and the references therein) and, with some reservations, as small as 8 μm.[14] Blood can behave like a fluid whose non-Newtonian characteristics become relevant when subjected to very small shear-strain rates. These shear-strain rates become relevant in small diameter vessels, particularly in capillaries wherein RBCs move in a single file. Our model does not deal with transport in this region because we consider the capillary bed to be part of the nutrient microcirculation.[23] We therefore treat blood as an incompressible homogeneous Newtonian fluid for the remaining larger vessels in the microcirculation.[27]

Based on values of the Reynolds (Re) and Stokes (Stk) numbers, we also assume blood flow to be laminar. Specifically, $\mathrm{Re} < 1000$ for large arteries and smaller vessels,[27,42] with typical values reported in Table 1. The Stokes number, $\mathrm{Stk} = \rho_{\mathrm{RBC}} d_{\mathrm{RBC}}^2 v/(36\mu a)$, describes the tendency of a particle suspended in flow to diverge from the streamlines. Here $\rho_{\mathrm{RBC}} = 1080$ kg/m^3 is the density of an RBC, $d_{\mathrm{RBC}} = 6.2 - 8.2\,\mu$m is the RBC diameter, v is the cross sectionally averaged velocity of whole blood, μ is the blood viscosity, and a is the vessel radius. Particles with a $\mathrm{Stk} > 1$ are inertially driven, while particles with $\mathrm{Stk} \ll 1$ follow the streamlines. For the arterioles considered in this study (see Table 3 below), $\mathrm{Stk} < 10^{-5}$.

Finally, we assume that the flow is steady and that axial perturbations are negligible. While unrealistic for large vessels in which the temporally periodic flow effects generated by the heart are noticeable,[56] this assumption is reasonable for smaller vessels in which the flow stabilizes and becomes well mixed.[27] Since flow in arterioles is stable, we ignore the effects of wall deformation and model the arteriolar vessels as straight cylindrical rigid walled tubes (Fig. 1).

Under these assumptions, flow velocity has a parabolic profile given by the Poiseuille law. An alternative, which is equally amenable to the analytical treatment presented below, is to treat blood in microcirculation as an inhomogeneous continuum fluid consisting of an RBC rich core and a cell-free layer; this approximation would result in a velocity profile that is more blunt than its parabolic counterpart (Ref. 48 and the refer-

TABLE 1. Typical Reynolds numbers for several levels of blood vessels in a network, as reported in Ref. 17.

Level	Vessel description	Reynolds number
1	Aorta	1700
2	Large arteries	130
3	Main branches	30
8	Arterioles	0.02
9	Capillaries	0.004

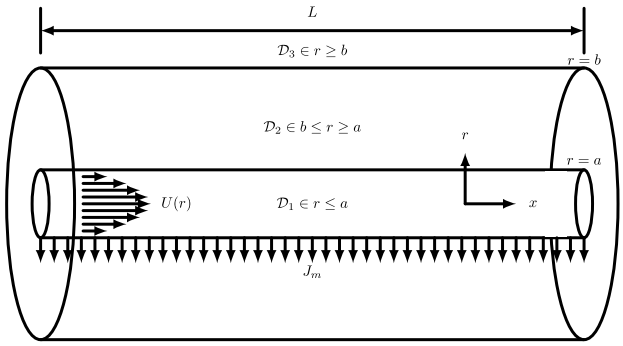

FIGURE 1. Schematic representation of blood flow in a vessel with diffusive losses to the surrounding tissue.

ences therein). Likewise, treating blood as a non-Newtonian fluid would flatten the parabolic (Poiseuille) velocity profile; the model presented below can be readily augmented to account for this effect.

For the range of flow velocities relevant to our study, significant O_2 losses are not observed prior to blood arriving at the arteriolar tree.[35,50] In addition to relatively high velocities and large arterial diameters, this could be due to the increase in wall thickness for larger vessels, which decreases the effective radial diffusion coefficient of the surrounding tissue.[16] Hence, the O_2 loss from the circulation becomes significant when blood transits through the arteriolar circulation, during which a significant portion of O_2 contributes to the re-oxygenation of venous blood[24] rather than to tissue oxygenation.[23] These findings suggest that a model of D_{O_2} through a single arteriole has a sufficient explanatory power to describe the effects of changes in Hct over the entire arterial tree.

Approximately 98% of O_2 carried by whole blood is bound to hemoglobin in RBCs,[36] which increases the amount of O_2 transported per blood unit. The concentration of RBC-bound O_2 is nonlinearly proportional to the concentration of O_2 in plasma. This relationship is described by the O_2-hemoglobin dissociation curve, $S_{O_2} = S_{O_2}(P_{O_2})$, that relates the O_2 saturation of RBCs, S_{O_2}, to the O_2 partial pressure, P_{O_2}[36]; this framework assumes that the local P_{O_2} in both plasma and RBCs are in equilibrium.[19,32,33] The nonlinear relationship $S_{O_2} = S_{O_2}(P_{O_2})$ often takes a sigmoidal form, which is described either analytically[2,21] or by tabulated experimental values.[55] For the range of O_2 saturations, $10\% < S_{O_2} < 95\%$, we approximate the O_2-hemoglobin dissociation curve in Ref. 1 with a spline

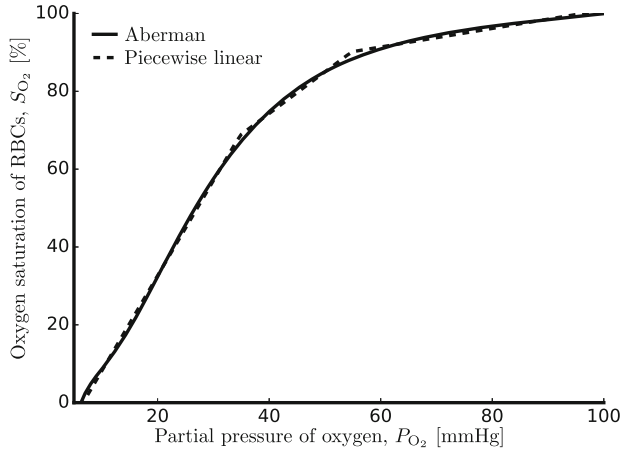

FIGURE 2. The oxygen-hemoglobin saturation curve[1] and its three-piece linear least-squares-fit approximation. This comparison demonstrates the accuracy of the piecewise linear representation (2) of the sigmoidal dissociation curve $S_{O_2} = S_{O_2}(P_{O_2})$ from Ref. 1.

$$S_{O_2} = \sum_{k=0}^{7} A_{k+1} \left(\frac{P_{O_2} - 27.5}{P_{O_2} + 27.5} \right)^k . \tag{1}$$

The coefficients $A_1 = 51.87074$, $A_2 = 129.8325$, $A_3 = 6.828368$, $A_4 = -223.7881$, $A_5 = -27.95300$, $A_6 = 258.5009$, $A_7 = 21.84175$, and $A_8 = -119.2322$ are determined in Ref. 1 by a least-squares fit of data on Hb with pH = 7.4, at a temperature of 37°C. Our local linear approximation of this relation is

$$S_{O_2} = a_1 + a_2 P_{O_2}, \tag{2a}$$

wherein P_{O_2} is expressed in mmHg, and

$$a_1 = \begin{cases} -16.22797 & 5.0 \leq P_{O_2} \leq 35.0 \\ 31.47615 & 35.0 \leq P_{O_2} \leq 55.0 \\ 77.09654 & 55.0 \leq P_{O_2} \leq 95.0 \end{cases}, \qquad a_2 = \begin{cases} 2.44297 & 5.0 \leq P_{O_2} \leq 35.0 \\ 1.07043 & 35.0 \leq P_{O_2} \leq 55.0 \\ 0.23817 & 55.0 \leq P_{O_2} \leq 95.0 \end{cases}. \tag{2b}$$

Figure 2 demonstrates the agreement between this approximation and the sigmoidal model in Ref. 1.

Unlike for other solutes in the blood stream, the equilibrium of O_2 in the surrounding tissue and in the blood is governed by P_{O_2} [mmHg] rather than by the total O_2 concentration in blood, C [mL_{O_2}/L_{blood}]. The latter is given by[39]

$$C = k_1 \mathrm{Hb} \frac{S_{O_2}}{100} + k_2 P_{O_2}, \tag{3}$$

where $k_1 = 1.39\,\mathrm{mL_{O_2}/g_{Hb}}$ is the Hufner constant, $k_2 = 0.03066\,\mathrm{mL_{O_2}/(L_{blood}\ mmHg)}$ is the solubility of O_2 in plasma, Hb $[\mathrm{g_{Hb}/L_{blood}}]$ is the concentration of hemoglobin. Since O_2 is carried by hemoglobin whose concentration is $\mathrm{Hb} = \mathrm{Hct}/0.3$,[39] combining (2) and (3) yields $C = k_1\mathrm{Hct}(a_1 + a_2 P_{O_2})/30 + k_2 P_{O_2}$ or

$$P_{O_2} = \frac{C - k_1 a_1 \mathrm{Hct}/30}{k_1 a_2 \mathrm{Hct}/30 + k_2}. \tag{4}$$

Consistent with the treatment of blood in microcirculation as a continuum, we adopt a continuum representation of O_2 transport, which is based on an advection-reaction-diffusion (ARD) equation. Such a formulation assigns a single effective diffusion coefficient to O_2 that both diffuses in plasma and is transported by hemoglobin (Refs. 14; 40, p. 801). The reaction terms in the ARD equations (see Appendix A) represent oxygen consumption in both a blood vessel and the surrounding tissue; we later show that oxygen consumption in the blood vessel is negligible, and this term is set to zero in the corresponding ARD. Oxygen consumption in tissue can be described by Michaelis–Menten kinetics,[14]

$$\kappa_2(P_{O_2}) = \frac{\kappa_2^{\max} P_{O_2}}{P_{O_2} + P_{O_2}^{\mathrm{crit}}}, \tag{5}$$

with $0.5 \le P_{O_2}^{\mathrm{crit}} \le 1.0$[14] and $P_{O_2} = 23.5 \pm 5.3$ mmHg in capillary tissue.[23] This kinetics law is typically used in cases of extreme hypoxia. When tissue $P_{O_2} \gg P_{O_2}^{\mathrm{crit}}$, the reaction is approximately zeroth-order, i.e., the rate κ_2 is approximately constant.[6,14,38] Our analysis deal with small deviations from the normal state, which renders the approximation $\kappa_2 = \text{constant}$ adequate. (Conversely, if $P_{O_2} \ll P_{O_2}^{\mathrm{crit}}$ then the reaction rate can be treated as linear first order. For a development of the first-order reaction kinetics see Ref. 58.)

Finally, we assume that two processes are responsible for the O_2 loss from the arteriolar vessels: its consumption in tissue and its adsorption into surrounding venules. Since the spatial distribution of venules around arterioles is seemingly random, we model their combined effect by introducing an average radius of adsorption. We prescribe a fixed concentration boundary condition at the average venule location radius. (If the oxygen consumption rate in tissue were high and the steady state P_{O_2} in tissue were lower than the steady-state P_{O_2} in the venules, the venules would act as a source of O_2 instead of a sink. However, we do not address the change in oxygen consumption in tissue and in the nutrient microcirculation. Instead we focus on the more likely case where venules absorb O_2.)

Model Formulation

Blood Flow

Blood flow velocity $u(r)$ is assumed to follow the Poiseuille (parabolic) law. The corresponding cross-sectionally averaged flow velocity v in a vessel of radius a is given by

$$v = \frac{a^2 \Delta P}{8 \mu L}, \tag{6}$$

where ΔP is the pressure drop along the vessel of length L, and the dynamic blood viscosity μ is primarily dependent on the concentration of RBCs in whole blood; we neglect its dependence on other factors, e.g., temperature and other suspended particles. (Note that our analysis is applicable to other constitutive models of blood, e.g., those resulting in blunter flow profiles discussed in "Physiological Considerations" section, for which v is linearly proportional to the pressure gradient $\Delta P/L$.) Since our analysis focuses on anemic conditions, we use the relation (Ref. 59 and the references therein)

$$\mu = 1.22 + 0.00675 \times \mathrm{Hct} + 0.00208 \times \mathrm{Hct}^2 \tag{7}$$

to describe this dependence.

Oxygen Transport in a Vessel and the Surrounding Tissue

Transport of O_2 in a vessel and the surrounding tissue is described by two advection-diffusion-reaction equations, one for the vessel and one (with the advective velocity set to zero) for the tissue. These equations are coupled by enforcing the continuity of both the partial pressure of oxygen, P_{O_2}, and the oxygen mass flux at the vessel's wall (a detailed problem formulation is provided in Appendix A). This formulation does not require *a priori* knowledge of the diffusive losses (flux) through the vessel's wall. Instead this quantity is found as part of the problem's solution. While the diffusion term in the ARD equation for the vessel is typically much smaller than the advective term, we keep them both for completeness.

A typical arteriole has length $0.1\ \mathrm{cm} \le L \le 1.2\ \mathrm{cm}$ and radius-to-length ratio $0.0033 \le a/L \le 0.0075$.[3,35,57] Diffusion coefficients of O_2 in blood and tissue are $D_1 \approx 2.0 \times 10^{-4}\ \mathrm{cm^2/s}$[15,20] and $10^{-6}\ \mathrm{cm^2/s} \le D_2 \le 10^{-5}\ \mathrm{cm^2/s}$,[35] respectively. Average blood velocity in arterioles is $0.22\ \mathrm{cm/s} \le v \le 1.0\ \mathrm{cm/s}$,[35] giving rise to the dispersivity coefficient $1.29 \times 10^{-4}\ cm \le \alpha \le 1.6 \times 10^{-2}$ cm. The reaction rate constants for O_2 scavenging in normal blood and tissue are $\kappa_1 \approx 0.0\,\mathrm{mL_{O_2} cm^{-2} s^{-1}}$[11] and $\kappa_2 \le 2.19 \times 10^{-7}\,\mathrm{mL_{O_2}\ cm^{-2}\ s^{-1}}$,[49] respectively. Thus, the reaction rate in the

blood, κ_1, is negligible in comparison to the rates of advection and diffusion, and we set $\kappa_1 = 0$. Since the Michaelis-Menton kinetics in the tissue exist under normal conditions in the zeroth-order regime, we treat the reaction rate constant in the tissue, κ_2, as constant. (The reaction rate κ_1 may be non-negligible in blood with an elevated concentration of leukocytes, as they are the primary cause of O_2 consumption in blood, but this is not a physiological condition of interest in this study.)

Analytical Solution

For a blood vessel of length L ($0 \le x \le L$), we show in Appendix B that $C(r, x)$, the O_2 concentration in the tissue ($a \le r \le b$), is related to $C_{av}(x)$, the cross-sectionally averaged O_2 concentration in the vessel ($0 \le r \le a$), by

$$C(r,x) = [\alpha_1 C_{av}(x) + \alpha_2]\ln\left(\frac{r}{b}\right) + \alpha_3 \ln\left(\frac{a}{r}\right) - \frac{\kappa_2 r^2}{4D_2}, \quad a \le r \le b, \quad 0 \le x \le L. \tag{8}$$

with

$$C_{av}(x) = \gamma + \beta_1 e^{\gamma_+ x} + \beta_2 e^{\gamma_- x}, \quad 0 \le x \le L. \tag{9}$$

All the constants in these expressions are defined in Appendix B in terms of the vessel geometry (the radii a and b and the length L), the transport characteristics (the flow velocity v, the diffusion coefficients D_1 and D_2, the reaction rate κ_2), and the prescribed O_2 concentrations, c_0 and c_L, at the vessel's inlet ($x = 0$) and outlet ($x = L$), respectively.

In a network analysis the parent vessel outflow boundary condition may be defined as the inflow boundary condition for the respective daughter vessels. However, at the end of the terminal vessels an outflow boundary condition must be assumed. We approximate the terminal vessel outflow condition as unimpeded flow represented by a semi-infinite vessel of the same diameter as the parent vessel. As a first-order approximation of the network conditions, we consider a semi-infinite vessel, which yields

$$C_{av}(x) = \gamma + (c_0 - \gamma)e^{\gamma_- x}, \quad 0 \le x \le \infty. \tag{10}$$

Consequently, when the outflow boundary condition for the finite vessel is set equal to the inflow condition of the semi-infinite vessel, the solution simplifies to a semi-infinite vessel where the region of interest is $0 \le x \le L$.

The oxygen delivery D_{O_2} is defined as the total O_2 delivered per unit time, and is found as the product of the O_2 concentration in the bloodstream and the volumetric flow rate,

$$D_{O_2} = C_{av}\frac{a^2 \pi v}{2}. \tag{11}$$

Model Parametrization

The diffusion coefficient of O_2 in plasma ranges between 1.20×10^{-5} cm^2/s and 1.62×10^{-5} cm^2/s for temperature 25 and 37°C, respectively.[15] The same study reported the range for whole blood to be between $D_1 = 1.62 \times 10^{-5}$ cm^2/s at 25°C and $D_1 = 2.18 \times 10^{-5}$ cm^2/s at 37°C. Another experimental study[20] put the value of D_1 in whole blood in the range 0.8×10^{-5} cm^2/s $\le D_1 \le 2.1 \times 10^{-5}$ cm^2/s, and used a least-squares fit to their data to estimate a linear relationship between D_1 and Hct,

$$D_1 = 10^{-5} \times (1.98 - 0.0085 \times \text{Hct})\ \text{cm}^2/\text{s}, \tag{12}$$

which we use in the simulations reported below.

Values of the O_2 diffusion coefficient in tissue were reported to range between $D_2 = 1.1 \times 10^{-4}$ cm^2/s and 4×10^{-8} cm^2/s.[28] This range of values is unrealistic at the lower extreme and considering the full range of values would introduce too great of an uncertainty for useful observations. Therefore, we narrow this range, such that a realistic hypothesis can be developed. We start by noting that the O_2 diffusion coefficient in water varies between 1.5×10^{-5} cm^2/s and 4.5×10^{-5} cm^2/s.[18] As striated muscle tissue is approximately 70% water,[13] the values $D_2 < 10^{-6}$ cm^2/s are unrealistic for a majority of tissue surrounding arterioles. Moreover, the values of $D_2 > 2 \times 10^{-5}$ cm^2/s are based on fitting data to a mathematical model.[37] Therefore, we suggest that values beyond the range of 10^{-6} cm^2/s $\le D_2 \le 10^{-4}$ cm^2/s should be heavily scrutinized and values of D_2 in human tissue are of the same order of magnitude as the values reported in Ref. 18 for free water. In the results presented below, we choose a median value of $D_2 = 10^{-5}$ cm^2/s.

Our model accounts for O_2 loss in the tissue due to O_2 shunting into the venule vasculature that runs parallel to the arterioles. Specifically, this O_2 sink is represented by the fixed concentration boundary condition at the tissue radius $r = b$, whose value is estimated from the following considerations. The P_{O_2} measurements from vessels and tissue around the microcirculation[53] point to a relationship between the arteriole diameter and P_{O_2} in A1-A4 arterioles (Table 2). (As a disclaimer, we note that venules do not necessarily exhibit similar behavior.) However, venular P_{O_2} may increase as flow returns to the venous vas-

TABLE 2. Arteriole, venule, and interstituim hamster tissue P_{O_2}, as reported in Ref. 53.

Vessel/Tissue	P_{O_2} [mmHg]	Diameter, $2a$ [μm]	RBC velocity, v [cm/sec]
A1	51.0 ± 9.8	64.3 ± 20.0	0.58 ± 0.35
	[32.3–80.6]	[25.0–120.0]	[0.07–1.60]
A2	44.1 ± 9.1	31.6 ± 12.1	0.32 ± 0.21
	[20–71.5]	[8.6–67.2]	[0.4–1.12]
A3	39.9 ± 9.2	13.4 ± 5.5	0.22 ± 0.11
	[21.7–58.0]	[7.2–28.9]	[0.08–0.55]
A4	34.0 ± 7.9	7.7 ± 2.4	0.14 ± 0.09
	[21.9–55.5]	[3.7–11.5]	[0.04–0.45]
Venules	30.8 ± 10.8	65.5 ± 38.0	0.07 ± 0.05
	[1.7–55.5]	[10.6–201.5]	[0.02–0.31]
Tissue	24.6 ± 5.8	–	–
	[11.1-36.0]	–	–

culature due to arteriole-venule O_2 shunting.[7,23] Moreover, venules may both supply and absorb O_2 from the surrounding tissue,[7] which aids in the maintenance of a homogeneous distribution of P_{O_2} in tissue. The values of P_{O_2} reported in Table 2 are used to compute the inlet O_2 concentration, c_0, by using the equation leading to (4).

Since the tissue measurements in Ref. 53 were taken at least 20 μm from any arteriole, we estimate their location to be approximately $3a$ away from the respective arteriole. The measured average capillary path length in pulmonary tissue in cats is 0.0556 ± 0.0285 cm.[44] Thus we assume that the average distance between arterioles and the surrounding venules is 0.0556 cm. Therefore the radius b (in cm) is $b = a + 0.0556$.

The rate of O_2 loss through the vessel walls is represented by the diffusive flux $J_m = -D_2 \partial_r C(a, x)$ and the resulting D_{O_2} is computed for the following values of the model parameters. The resting rate of O_2 consumption in tissue is $\kappa_2 \approx 2.17 \times 10^{-7}\,\mathrm{mL_{O_2}/(cm^2 s)}$.[49] While the value of κ_2 is directly affected by the metabolism of the tissue cells and the tissue metabolism may increase when the tissue is engaged in increased activity, most tissue spends a majority of its time in a sedentary state during blood transfusion, allowing us to ignore this phenomenon.

For given arteriole length L and radius a and average flow velocity $v = v(\mathrm{Hct} = 45\%)$, the pressure gradient $\Delta P/L$ is computed from (6). We assume that the pressure gradient values, which are reported in Table 3, remain unaffected by Hct changes. Then, $v = v(\mathrm{Hct})$ is computed from (6) by using the viscosity-hematocrit relation, $\mu = \mu(\mathrm{Hct})$, in (7). The fifth column is the calculation of the pressure gradient along the arterioles based on solving equation (6) while assuming normal hematocrit (Hct = 45%).

RESULTS

We use our model to investigate the effects of changing Hct on oxygen delivery in the microcirculation. Figure 3 exhibits the model's prediction of the dependence on hematocrit of oxygen delivery to arteriole outlet, $D_{O_2} = D_{O_2}(\mathrm{Hct})$, normalized with its counterpart at Hct = 45%. The latter value represents an average Hct in the arterioles; its distribution across the arteriolar network is heterogeneous and may be as high as 50% in some arterioles. It is worthwhile emphasizing that an increase in Hct does not affect the graph in Fig. 3 and would only minimally affect the curves in Fig. 4 by shifting the normalization value without changing the curves' shape. The D_{O_2} vs. Hct curves for the four arteriole levels, whose geometric properties are collated in Table 3, are indistinguishable from each other in both Figs. 3 and 4 . The early part of the curve in Fig. 3 (up to Hct = 23%) exhibits the rise in D_{O_2} because the rise in Ca_{O_2}, computed with (3) for $S_{O_2} = 98\%$, dominates the increases in both the residence time L / v and the blood viscosity μ. Above Hct = 23%, D_{O_2} decreases reflecting the increase in residence time (the decrease in viscosity μ and, hence, velocity v), which translates into the rising O_2 diffusive loss through the walls.

Martini *et al.*[29] measured the effects of vasodilation for up to two hours post transfusion. The largest changes were observed at 60 min post transfusion, after which time the vessels started to return to their normal state. At 60 min post-transfusion, the arteriolar diameter increased, on average, by 10%, and the RBC velocity increased, on average, by 24%. These changes due to vasodilation are not reflected in the D_{O_2} vs Hct curve in Fig. 3 because it is obtained with a steady-state model (see Appendix A). This modeling choice is justified by the following consideration. While the vasodilation of the arteriolar network is a transient

TABLE 3. Values of the arteriolar network vessel dimensions and hydraulic characteristics used in our simulations.

Arteriole	P_{O_2} (mmHg)	v(Hct = 45%) (cm/s)	L (cm)	2a (mm)	$(\Delta P)/L$ (Pa/cm)
A1	70.0	0.97	1.2	0.08	7.75
A2	55.0	0.62	0.6	0.05	7.92
A3	45.0	0.39	0.2	0.03	8.29
A4	40.0	0.22	0.1	0.015	9.31

The values in columns 2 through 5 are taken from Ref. 35 and roughly represent the averages of their counterparts in Table 2; the pressure gradient values in column 6 is computed from the corresponding values of v using (6) and are assumed not to vary with Hct.

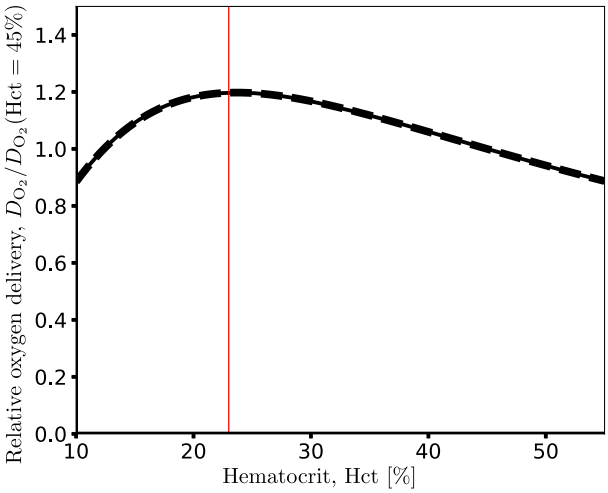

FIGURE 3. Impact of hematocrit changes on oxygen delivery at an arteriole's outlet, normalized with its reference (pre-transfusion) value at Hct = 45%, D_{O_2}/D_{O_2}(Hct = 45%). The early part of the curve (up to Hct = 23%, i.e., to the left of the vertical red line) exhibits a rise in D_{O_2} because the increase in Ca_{O_2} dominates those in both the residence time and the blood viscosity. Above Hct = 23%, D_{O_2} decreases reflecting the increase in residence time (the decrease in viscosity μ and, hence, velocity v), which translates into the rising O_2 diffusive loss through the walls.

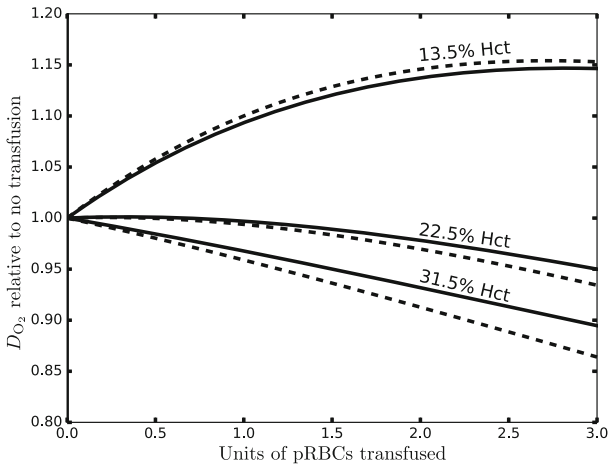

FIGURE 4. Relative D_{O_2} at the arteriole's outlet vs. units of pRBCs transfused for the pre-transfusion Hct deficits of 30, 50, and 70%, which corresponds to Hct = 31.5, 22.5, and 13.5%, respectively. Each solid/dashed line pair represents a different pre-transfusion Hct. Transfusion of three units in severe anemia (13.5% Hct) increases D_{O_2} by only 17.5% over the anemic condition. Our results are in close agreement with the previous study[59] (dashed lines), which prescribed the diffusional O_2 loss observed in the microcirculation in the hamster window chamber preparation.[23]

phenomenon, the time scale on which the vessel and flow parameters change is large in comparison with the time scale on which O_2 transits through an arteriole.

Figure 4 shows the change in D_{O_2}, reported as the ratio between the post- and pre-transfusion levels of D_{O_2} (the curve labels refer to the pre-transfusion Hct), in response to transfusion of 0.0–3.0 units of pRBCs. The pre-transfusion anemic state is reported as % of normal Hct, such that 50% Hct indicates a deficit of 50% in RBC concentration, or Hct = 23% for an individual whose normal Hct is 45%. Addition of RBCs to the circulation for virtually all conditions of anemia decreases D_{O_2} because the increased viscosity and residence time of RBCs in the arteriole have a greater effect on D_{O_2} than does the increase in Ca_{O_2}. The results reported in Fig. 4 are visually identical for the four arteriole sizes reported in Table 3.

Blood transfusions increase the volume of blood in the circulatory system. However, this effect is transient and hypervolemia due to transfusion abates as blood volume returns to normovolemic. This process is extraordinarily quick in comparison to the time required for the body to reproduce RBCs. Blood plasma is 92% water, and is easily re-absorbed by the body. The rate of plasma re-absorption post transfusion in patients is not precisely known. However, blood transfusions are performed slowly to allow for plasma re-absorption and/or venous filling. It has been suggested that the venous structure may stretch to accommodate small changes in blood volume. In our analysis we assume steady-state D_{O_2} once the circulation returns to its normovolemic condition. Specifically, the post-transfusion Hct is calculated as[59]

$$\mathrm{Hct}_{\mathrm{post}} = \frac{\mathrm{Hct}_{\mathrm{pre}} V_{\mathrm{pre}} + n\mathrm{Hct}_{\mathrm{pRBC}} V_{\mathrm{pRBC}}}{V_{\mathrm{pre}} + nV_{\mathrm{pRBC}}}, \quad (13)$$

where $\mathrm{Hct}_{\mathrm{pre}}$ is the Hct before transfusion, $\mathrm{Hct}_{\mathrm{pRBC}}$ is the pRBC Hct, V_{pRBC} is the pRBC volume, V_{pre} is

the normovolemic volume of blood in the circulation before transfusion, and n is the number of units transfused. In our simulations we set $V_{\text{pre}} = 5$ liters, $V_{\text{pRBC}} = 0.3$ liters, and $\text{Hct}_{\text{pRBC}} = 65\%$. However, post-transfusion blood is initially hypovolemic in anemic patients, becoming normovolemic in time. Thus (13) is only correct shortly after transfusion. As fluid is re-absorbed by the body returning the blood volume to normovolemic conditions,[51] (13) becomes

$$\text{Hct}_{\text{post}} = \text{Hct}_{\text{pre}} + \frac{n\text{Hct}_{\text{pRBC}} V_{\text{pRBC}}}{V_{\text{pre}}}. \quad (14)$$

The dashed lines in Fig. 4 represent the results from Ref. 59, wherein the relationship between the pre- and post-transfusion levels of D_{O_2} assumes a constant 14% loss of O_2 over the length of the network, such that

$$\frac{D_{O_2,\text{post}}}{D_{O_2,\text{pre}}} = \frac{\mu_{\text{pre}}}{\mu_{\text{post}}} \frac{\text{Hct}_{\text{post}} - 0.14\mu_{\text{post}}^2}{\text{Hct}_{\text{pre}} - 0.14\mu_{\text{pre}}^2}. \quad (15)$$

Our model makes no such assumption. Figure 4 demonstrates that blood transfusions provide no increase in D_{O_2} unless the Hb deficit is $> 50\%$. Furthermore, transfusion of 3 units of pRBCs in severe anemia (13.5% Hct) increases D_{O_2} by only 17.5% over the anemic condition. The present study correlates extraordinarily well with Ref. 59, where the diffusional O_2 loss was derived by an empirical correction based on the results from P_{O_2} distribution in the microcirculation in the hamster window chamber preparation.[23] These results are supported by the studies showing that D_{O_2} in humans increases as Hct decreases to 30–33%,[31,34] which requires the maintenance of blood pressure to support the necessary increase in blood flow.

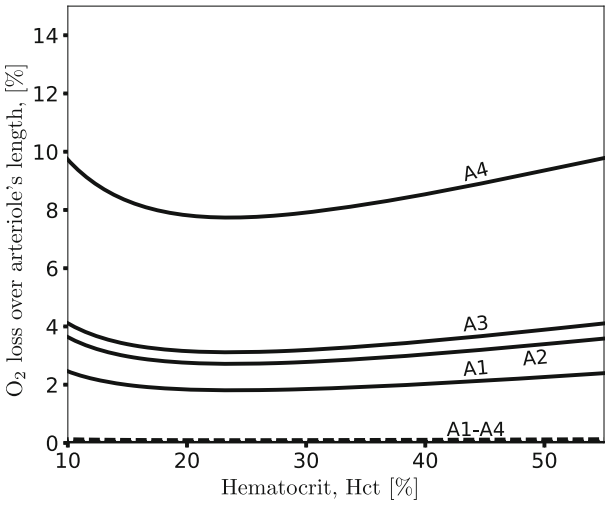

FIGURE 5. O_2 deficit at arteriole outlet (relative to arteriole inlet) vs. Hct. The O_2 losses increase as the vessel diameter decreases (diameters of the arterioles A1–A4 are given in Table 2). The solid and dashed lines correspond to the upper ($D_2 = 10^{-4}$ cm^2/s) and lower ($D_2 = 10^{-6}$ cm^2/s) bounds of the oxygen diffusion coefficient in tissue, respectively.

Figure 5 shows the percentage of O_2 entering the vessel that is lost through the vessel wall for each class of arterioles described in Table 3. The solid and dashed lines correspond to the upper ($D_2 = 10^{-4}$ cm^2/s) and lower ($D_2 = 10^{-6}$ cm^2/s) bounds of the oxygen diffusion coefficient in tissue, respectively. It has been suggested[12] that the O_2 losses in the arterioles are in the range of 20–30% over the length of the entire arteriolar network. Figure 5 reveals that such losses are consistent with $D_2 \approx 10^{-5}$ cm^2/s. This figure also demonstrates that the O_2 losses increase as the vessel radius decreases; this is to be expected, as the blood draws nearer to the nutritional microcirculation. Unlike the oxygen delivery (Figs. 3 and 4), the amount of O_2 that diffuses out of the vessel wall varies with the arteriole size.

DISCUSSION

There is considerable debate as to whether blood transfusion is beneficial, and at what RBC deficit it is necessary. Most transfusions are done when hemoglobin reaches approximately 50% of normal to avoid the possibility of focal hypoxia due to inhomogeneous distribution of blood flow in the tissue. Our mechanistic analysis supports the experimental evidence that using blood transfusion to treat anemia reduces D_{O_2}, unless the deficit is Hct $> 50\%$ (blood Hb < 6.1 g/dL) regardless of the number of units transfused. This effect indicates that the increase in blood viscosity outweighs the benefit of increased Ca_{O_2}, which ultimately decreases the quantity of O_2 arriving to the nutritional microcirculation.

Our analysis ignores the effects that blood transfusion may have on the circulation as a whole or on cardiac function. Yet, it clearly demonstrates that since changes in blood viscosity significantly affect O_2 transport, positive effects that may increase D_{O_2} over that in the anemic state must first overcome the viscosity-related negative effects. Our study shows that transfusing pRBCs to anemic patients lowers O_2 delivery to the microcirculation, and is therefore counterproductive. There may be long-term beneficial effects due to the body's response to blood transfusion. However, they are unlikely to manifest themselves in the short term. On the quantitative/prescriptive level, our work suggests that transfusion of pRBCs in anemic patients should only be considered when hemoglobin levels are below 55% of normal.

We have assumed that blood pressure does not change due to blood transfusion, which is consistent

with clinical experience, although this effect has not been systematically studied. This phenomenon may in part explain the beneficial anomalous effect associated with blood transfusion, by which a significant segment of transfused anemic individuals feel improvement after the procedure, even though our studies suggest that the opposite should occur. The presence of counteracting beneficial effects could be associated with the reduction of peripheral vascular resistance thorough vasodilation that overcompensates the increase due to increased blood viscosity. Evidence for such an effect was found in Ref. 29, where both a significant reduction of blood pressure and a significant increase in cardiac output were observed when Hct and blood viscosity were increased by blood transfusion in awake hamsters. Clinical hemodynamic studies before and after transfusion in anemic individuals could provide important insights on how to optimize blood transfusion regimes.

Our mathematical analysis is based on a number of simplifying assumptions. While we treated blood in the microcirculation as a homogeneous Newtonian fluid, our analysis is equally applicable to other constitutive models that result in blunter flow velocity profiles, as long as the cross-sectionally averaged flow velocity remains linearly proportional to the pressure drop across an arteriole's length. Relevant examples treat blood as an inhomogeneous shear-thinning fluid (e.g., Ref. 47 and the references therein) or as a mixture of two Newtonian fluids (e.g., Ref. 46 and the references therein). Another improvement upon our model would be to go beyond an average (constant) Hct by accounting for heterogeneous Hct distribution throughout the entire arteriolar network. The latter can be calculated with, e.g., a model reported in Ref. 45.

Our study has important clinical implications. The current practice of blood transfusion assumes that the only effect of adding RBCs to the circulation is to increase oxygen carrying capacity, and therefore increase oxygen delivery. Peak efficiency of oxygen delivery occurs in the anemic state at Hct 22%. This is a value usually associated with the so called "transfusion trigger". Adding a unit of blood at this point (pRBCs Hct 66%) causes a decrease in O_2 delivery of 0.02% and is progressively negative as more units of pRBCs are added. Therefore our results suggest that optimal blood management is associated with transfusing enough units up to reaching maximal O_2 delivery, a practice that although somewhat complex to implement would result in both substantial blood savings and improved O_2 delivery.

APPENDIX A: MATHEMATICAL MODEL OF OXYGEN TRANSPORT

Consider a simulation domain $\mathcal{D}$ that consists of two non-overlapping subdomains $\mathcal{D}_1$ and $\mathcal{D}_2$. The interface separating $\mathcal{D}_1$ from $\mathcal{D}_2$ is denoted by Γ. The O_2 concentration $C(\mathbf{x})$ is described by a solution of a system of linear steady-state ARD equations

$$0 = -\nabla \cdot \mathbf{J} - \kappa_i(C), \quad \mathbf{J} = -D_i \nabla C + \mathbf{u}_i C, \quad \mathbf{x} \in \mathcal{D}_i, \quad i = 1,2 \tag{16}$$

where $D_i > 0$ are the diffusion coefficients, $\mathbf{u}_i$ are the advective velocities, $\mathbf{J}$ is the advection-diffusion flux, and $\kappa_i(C)$ are the rate laws of oxygen consumption. These equations are coupled by enforcing both the equilibrium of oxygen's partial pressure and the continuity of oxygen's mass flux across the interface Γ,

$$P_{O_2}(\mathbf{x}^-) = P_{O_2}(\mathbf{x}^+) \quad \text{and} \quad \mathbf{n} \cdot \mathbf{J}(\mathbf{x}^-) = \mathbf{n} \cdot \mathbf{J}(\mathbf{x}^+), \quad \mathbf{x}_\Gamma \in \Gamma, \tag{17}$$

where $\mathbf{n}(\mathbf{x}_\Gamma)$ is the unit normal vector to Γ at point $\mathbf{x}_\Gamma$; and $\mathbf{x}^-$ and $\mathbf{x}^+$ indicate the limits of C and $\mathbf{J}$ as $\mathbf{x} \to \mathbf{x}_\Gamma$ from inside subdomains $\mathcal{D}_1$ and $\mathcal{D}_2$, respectively. They are also subject to appropriate boundary conditions on the external boundary of $\mathcal{D}$, such as those given by (22) for the case where $\mathcal{D}_1$ represents a blood vessel and its external boundary reduces to two points: the vessel's inlet and outlet.

A blood vessel of radius a and length L ($a \ll L$) is represented by the domain $\mathcal{D}_1 = \{(r,x) : 0 \le r < a, 0 < x < L\}$, and the surrounding tissue by domain $\mathcal{D}_2 = \{(r,x) : a \le r < b, 0 < x < L\}$ (see Fig. 1). Then the ARD Eq. (16) take the form

$$0 = \frac{D_1}{r}\frac{\partial}{\partial r}\left(r\frac{\partial C}{\partial r}\right) + D_1\frac{\partial^2 C}{\partial x^2} - u(r)\frac{\partial C}{\partial x} - \kappa_1(C), \quad (r,x) \in \mathcal{D}_1 \tag{18a}$$

and

$$0 = \frac{D_2}{r}\frac{\partial}{\partial r}\left(r\frac{\partial C}{\partial r}\right) + D_2\frac{\partial^2 C}{\partial x^2} - \kappa_2(C), \quad (r,x) \in \mathcal{D}_2. \tag{18b}$$

The continuity conditions (17) at the interface $\Gamma = \{(r,x) : r = a, 0 \le x \le L\}$ become

$$\frac{C(a^-,\cdot) - k_1 a_1 \mathrm{Hct}/30}{k_1 a_2 \mathrm{Hct}/30 + k_2} = \frac{C(a^+,\cdot)}{k_3}, \qquad D_1\frac{\partial C}{\partial r}(a^-,\cdot) = D_2\frac{\partial C}{\partial r}(a^+,\cdot) \equiv -J_\mathrm{m}, \tag{19}$$

where k_3 is the solubility coefficient of O_2 in tissue (typically similar to k_2).

A1: Hydrodynamic Dispersion Approximation

Given the geometric constraint $a \ll L$, we are interested in the cross-sectionally averaged concentration in the blood vessel $\mathcal{D}_1$,

$$C_{\mathrm{av}}(x) = \frac{2}{a^2}\int_0^a C(r,x) r dr. \tag{20}$$

It follows from (18a) that the steady-state distribution of $C_{\mathrm{av}}(x)$ satisfies approximately an advection-reaction-dispersion equation[4,52]

$$0 = -\frac{2}{a}J_{\mathrm{m}} + D\frac{\partial^2 C_{\mathrm{av}}}{\partial x^2} - v\frac{\partial C_{\mathrm{av}}}{\partial x} - \kappa_1, \quad 0 < x < L \tag{21}$$

where $v \equiv 2a^{-2}\int_0^a u(r) r dr$ is the average flow velocity given by (6), $D = D_1 + \alpha v$ is the hydrodynamic dispersion coefficient with dispersivity $\alpha = a^2 v/(48 D_1)$, and $J_{\mathrm{m}}(z)$ is the (yet unknown) diffusive flux from the vessel into the surrounding tissue. This equation is subject to boundary conditions

$$C_{\mathrm{av}}(0) = c_0, \qquad C_{\mathrm{av}}(L) = c_L, \tag{22}$$

where c_0 and c_L are the (prescribed) O_2 concentrations at the vessel's inlet ($x = 0$) and outlet ($x = L$).

The interfacial continuity conditions (19) are replaced with a boundary condition for the O_2 concentration in the tissue. Thus, the reaction-diffusion equation (18b) is subject to the boundary conditions

$$C(a,x) = \varpi_1 C_{\mathrm{av}}(x) + \varpi_2, \qquad \varpi_1 = \frac{k_3}{(k_1 a_2 \mathrm{Hct}/30 + k_2)},$$
$$\varpi_2 = -\frac{k_1 a_1 k_3 \mathrm{Hct}}{(k_1 a_2 \mathrm{Hct} + 30 k_2)} \tag{23a}$$

and

$$C(b,x) = \varpi_1 c_b + \varpi_2, \quad \frac{\partial C}{\partial x}(r,0) = 0, \quad \frac{\partial C}{\partial x}(r,L) = 0. \tag{23b}$$

APPENDIX B: ANALYTICAL SOLUTION

For the physiological conditions discussed in "Oxygen Transport in a Vessel and the Surrounding Tissue" section, $\kappa_1 = 0$ and $\kappa_2 = \text{constant}$.

B1: Oxygen Concentration in the Tissue

Since under physiologically relevant conditions the O_2 concentration gradients in the tissue satisfy $\partial C/\partial x < \partial C/\partial r$, the leading-order (in a / L) approximation of (23) is

$$0 = \frac{D_2}{r}\frac{\partial}{\partial r}\left(r\frac{\partial C}{\partial r}\right) - \kappa_2, \quad a < r < b. \tag{24}$$

This equation is subject to the auxiliary conditions (23). The solution is

$$C(r,x) = \frac{A_1}{\ln(a/b)}\ln r + \frac{A_2}{\ln(a/b)} - \frac{\kappa_2 r^2}{4D_2}, \tag{25a}$$

where

$$A_1 = \varpi_{1,\mathcal{D}_1} C_{\mathrm{av}}(x) + \varpi_{2,\mathcal{D}_1} - \left(\varpi_{1,\mathcal{D}_3} c_b + \varpi_{2,\mathcal{D}_3}\right) + \frac{\kappa_2}{4D_2}\left(a^2 - b^2\right) \tag{25b}$$

$$A_2 = \left(\varpi_{1,\mathcal{D}_3} c_b + \varpi_{2,\mathcal{D}_3}\right)\ln(a) - \left(\varpi_{1,\mathcal{D}_1} C_{\mathrm{av}}(x) + \varpi_{2,\mathcal{D}_1}\right)\ln(b) + \frac{\kappa_2}{4D_2}\left(b^2\ln(a) - a^2\ln(b)\right). \tag{25c}$$

Rearranging the terms in this solution yields (8), in which the coefficients are given by

$$\alpha_1 = \frac{\varpi_{1,\mathcal{D}_1}}{\ln(a/b)}, \quad \alpha_2 = \frac{1}{\ln(a/b)}\left(\varpi_{2,\mathcal{D}_1} + \frac{\kappa_2 a^2}{4D_2}\right),$$
$$\alpha_3 = \frac{1}{\ln(a/b)}\left(\varpi_{1,\mathcal{D}_3} C_{\mathrm{b}} + \varpi_{2,\mathcal{D}_3} + \frac{\kappa_2 b^2}{4D_2}\right). \tag{26}$$

B2: Oxygen Concentration in the Vessel

The diffusive flux, from the vessel into the tissue, J_{m}, first defined in (21), is

$$J_{\mathrm{m}}(x) \equiv -D_2\frac{\partial C}{\partial r}(a,x). \tag{27}$$

It is expressed in terms of C_{av} by combining this expression with (25). Given this result, the solution of (21) with $\kappa_1 = 0$ is

$$C_{\mathrm{av}}(x) = \gamma + \frac{(\tilde{c}_0 - \gamma)e^{\gamma_-} - \tilde{c}_L + \gamma}{e^{\gamma_-} - e^{\gamma_+}} e^{\gamma_+ x} + \frac{\tilde{c}_L - (\tilde{c}_0 - \gamma)e^{\gamma_+} - \gamma}{e^{\gamma_-} - e^{\gamma_+}} e^{\gamma_- x}, \tag{28a}$$

where

$$\gamma = \frac{\frac{\kappa_2}{4D_2}\left(a^2\left(2\ln\left(\frac{a}{b}\right) - 1\right) + b^2\right) - \varpi_{2,\mathcal{D}_1} + \left(\varpi_{1,\mathcal{D}_3} c_b + \varpi_{2,\mathcal{D}_3}\right)}{\varpi_{1,\mathcal{D}_1}} \tag{28b}$$

and

$$\gamma_{\pm} = \frac{v}{2D} \pm \frac{\sqrt{v^2 - 4\beta D}}{2D}, \qquad \beta = \frac{2\varpi_{1,\mathcal{D}_1} D_2}{a^2 \ln\left(\frac{a}{b}\right)}. \tag{28c}$$

This is the same as (9) with

$$\beta_1 = \frac{(\tilde{c}_0 - \gamma)e^{\gamma_-} - \tilde{c}_L + \gamma}{e^{\gamma_-} - e^{\gamma_+}}, \qquad \beta_2 = \frac{\tilde{c}_L - (\tilde{c}_0 - \gamma)e^{\gamma_+} - \gamma}{e^{\gamma_-} - e^{\gamma_+}}. \tag{29}$$

B3: Semi-infinite Vessel

We redefine domains $\mathcal{D}_1$ and $\mathcal{D}_2$ as $\mathcal{D}_1 = \{(r,x) : 0 \le r < a, 0 < x < \infty\}$ and the surrounding tissue by $\mathcal{D}_2 = \{(r,x) : a \le r < b, 0 < x < \infty\}$. The ARD Eq. (21) with $\kappa_1 = 0$ and (24) are now supplemented with boundary conditions

$$C_{\mathrm{av}}(0) = c_0, \qquad C_{\mathrm{av}}(\infty) < \infty; \quad \text{and} \quad C(b,x) = c_b, \tag{30a}$$

respectively. The solution takes the form (10).

ACKNOWLEDGMENTS

This research was supported in part by National Science Foundation under Grant DMS-1802189.

REFERENCES

[1]Aberman, A., J. M. Cavanilles, J. Trotter, D. Erbeck, M. H. Weil, and H. Shubin. An equation for the oxygen hemoglobin dissociation curve. *J. Appl. Physiol.* 35(4):570–571, 1973.

[2]Adair, G. S. The hemoglobin system. VI. The oxygen dissociation curve of hemoglobin. *J. Biol. Chem.* 63(2):529–545, 1925.

[3]Adam, J. A. Blood vessel branching: beyond the standard calculus problem. *Math. Mag.* 84(3):196–207, 2011.

[4]Aris, R. On the dispersion of a solute in a fluid flowing through a tube. *Proc. Roy. Soc. London A* 235(1200):67–77, 1956.

[5]Beard, D. A., and J. B. Bassingthwaighte. Advection and diffusion of substances in biological tissues with complex vascular networks. *Ann. Biomed. Engrg.* 28(3):253–268, 2000.

[6]Beard, D. A., and J. B. Bassingthwaighte. Modeling advection and diffusion of oxygen in complex vascular networks. *Ann. Biomed. Engrg.* 29(4):298–310, 2001.

[7]Buerk, D. G., R. D. Shonat, C. E. Riva, and S. D. Cranstoun. O _2 gradients and countercurrent exchange in the cat vitreous humor near retinal arterioles and venules. *Microvasc. Res.* 45(2):134–148, 1993.

[8]Carson, J. L. Risk of anemia and transfusion triggers: implications for bloodless care. *Surg. Infect.* 6(S1):S17–S21, 2005.

[9]Crowell, J. W., R. G. Ford, and V. M. Lewis. Oxygen transport in hemorrhagic shock as a function of the hematocrit ratio. *Am. J. Physiol.* 196(5):1033–1038, 1959.

[10]Crowell, J. W., and E. E. Smith. Determinant of the optimal hematocrit. *J. Appl. Physiol.* 22(3):501–504, 1967.

[11]Daland, G. A., and R. Isaacs. Cell respiration studies: II. A comparative study of the oxygen consumption of blood from normal individuals and patients with increased leucocyte counts (sepsis; chronic myelogenous leucemia). *J. Exp. Med.* 46(1):53, 1927.

[12]Duling, B. R., and R. M. Berne. Longitudinal gradients in periarteriolar oxygen tension. A possible mechanism for the participation of oxygen in local regulation of blood flow. *Circ. Res.* 27(5):669–678, 1970.

[13]Forbes, R. M., A. R. Cooper, and H. H. Mitchell. The composition of the adult human body as determined by chemical analysis. *J. Biol. Chem.* 203(1):359–366, 1953.

[14]Goldman, D. Theoretical models of microvascular oxygen transport to tissue. *Microcirculation.* 15(8):795–811, 2008.

[15]Goldstick, T. K., V. T. Ciuryla, and L. Zuckerman. Diffusion of oxygen in plasma and blood. In Oxygen Transport to Tissue – II. Advances in Experimental Medicine and Biology, volume 75, edited by J. Grote, D. Reneau, and G. Thews. Springer, Boston, MA, 1976, p. 183.

[16]Gore, R. W. Wall stress: a determinant of regional differences in response of frog microvessels to norepinephrine. *Am. J. Physiol.* 222(1):82–91, 1972.

[17]Green, H. D. Circulation: physical principles. *Med. Phys.* 1:208–232, 1944.

[18]Harris, K. R., and L. A. Woolf. Pressure and temperature dependence of the self diffusion coefficient of water and oxygen-18 water. *Faraday Trans. 1: Phys. Chem. Cond. Phases* 76:377–385, 1980.

[19]Hellums, J. D., P. K. Nair, N. S. Huang, and N. Ohshima. Simulation of intraluminal gas transport processes in the microcirculation. *Ann. Biomed. Engrg.* 24(1):1–24, 1995.

[20]Hershey, D., and T. Karhan. Diffusion coefficients for oxygen transport in whole blood. *AIChE J.* 14(6):969–972, 1968.

[21]Hill, A. V. The possible effects of the aggregation of the molecules of haemoglobin on its dissociation curves. *J. Physiol. (Lond.)* 40:4–7, 1910.

[22]Intaglietta, M. Whitaker lecture 1996: Microcirculation, biomedical engineering, and artificial blood. *Ann. Biomed. Eng.* 25(4):593–603, 1997.

[23]Intaglietta, M., P. C. Johnson, and R. M. Winslow. Microvascular and tissue oxygen distribution. *Cardiovasc. Res.* 32(4):632–643, 1996.

[24]Ivanov, K. P., A. N. Derry, E. P. Vovenko, M. O. Samoilov, and D. G. Semionov. Direct measurements of oxygen tension at the surface of arterioles, capillaries and venules of the cerebral cortex. *Pflügers Arch.* 393(1):118–120, 1982.

[25]Klein, H. G., D. R. Spahn, and J. L. Carson. Red blood cell transfusion in clinical practice. *Lancet* 370(9585):415–426, 2007.

[26]Krogh, A. The rate of diffusion of gases through animal tissues, with some remarks on the coefficient of invasion. *J. Physiol.* 52(6):391, 1919.

[27]Lee, J.-S., and Y.-C. Fung. Flow in nonuniform small blood vessels. *Microvasc. Res.* 3(3):272–287, 1971.

[28]MacDougall, J. D. B., and M. McCabe. Diffusion coefficient of oxygen through tissues. *Nature* 215:1173–1174, 1967.
[29]Martini, J., A. G. Tsai, P. Cabrales, P. C. Johnson, and M. Intaglietta. Increased cardiac output and microvascular blood flow during mild hemoconcentration in hamster window model. *Am. J. Physiol. Heart Circ. Physiol.* 291(1):H310–H317, 2006.
[30]Mirhashemi, S., S. Ertefai, K. Messmer, and M. Intaglietta. Model analysis of the enhancement of tissue oxygenation by hemodilution due to increased microvascular flow velocity. *Microvasc. Res.* 34(3):290–301, 1987.
[31]Mori, K., H. Arai, K. Nakajima, A. Tajima, and M. Maeda. Hemorheological and hemodynamic analysis of hypervolemic hemodilution therapy for cerebral vasospasm after aneurysmal subarachnoid hemorrhage. *Stroke* 26(9):1620–1626, 1995.
[32]Nair, P. K., J. D. Hellums, and J. S. Olson. Prediction of oxygen transport rates in blood flowing in large capillaries. *Microvasc. Res.* 38(3):269–285, 1989.
[33]Nair, P. K., N. S. Huang, J. D. Hellums, and J. S. Olson. A simple model for prediction of oxygen transport rates by flowing blood in large capillaries. *Microvasc. Res.* 39(2):203–211, 1990.
[34]Pasipoularides, A. Optimal hematocrit: a Procrustean bed for maximum oxygen transport rate? *J. Appl. Physiol.* 113(3):353–354, 2012.
[35]Popel, A. S., and J. F. Gross. Analysis of oxygen diffusion from arteriolar networks. *Am. J. Physiol. Heart Circ. Physiol.* 237(6):H681–H689, 1979.
[36]Popel, A. S., and J. D. Hellums. Theory of oxygen transport to tissue. *Crit. Rev. Biomed. Eng.* 17(3):257, 1989.
[37]Popel, A. S., R. N. Pittman, and M. L. Ellsworth. Rate of oxygen loss from arterioles is an order of magnitude higher than expected. *Am. J. Physiol. Heart Circ. Physiol.* 256(3):H921–H924, 1989.
[38]Qiu, Y., and J. M. Tarbell. Numerical simulation of oxygen mass transfer in a compliant curved tube model of a coronary artery. *Ann. Biomed. Eng.* 28:26–38, 2000.
[39]Quintó, L., J. J. Aponte, C. Menéndez, J. Sacarlal, P. Aide, M. Espasa, I. Mandomando, C. Guinovart, E. Macete, and R. Hirt. Relationship between haemoglobin and haematocrit in the definition of anaemia. *Trop. Med. Int. Health* 11(8):1295–1302, 2006.
[40]Ress, D., J. K. Thompson, B. Rokers, R. K. Khan, and A. C. Huk. A model for transient oxygen delivery in cerebral cortex. *Front. Neuroenerget.* 1:3, 2009.
[41]Richardson, T. Q., and A. C. Guyton. Effects of polycythemia and anemia on cardiac output and other circulatory factors. *Am. J. Physiol.* 197(6):1167–1170, 1959.
[42]Sarpkaya, T. Experimental determination of the critical Reynolds number for pulsating Poiseuille flow. *J. Basic Eng.* 88(3):589–598, 1966.
[43]Shepherd, A. P., and G .L. Riedel. Optimal hematocrit for oxygenation of canine intestine. *Circ. Res.* 51(2):233–239, 1982.
[44]Sobin, S. S., Y.-C. Fung, R. G. Lindal, H. M. Tremer, and L. Clark. Topology of pulmonary arterioles, capillaries, and venules in the cat. *Microvasc. Res.* 19(2):217–233, 1980.
[45]Sriram, K., M. Intaglietta, and D. M. Tartakovsky. Hematocrit dispersion in asymmetrically bifurcating vascular networks. *Am. J. Physiol. Heart Circ. Physiol.* 307(11):H1576–H1586, 2014.
[46]Sriram, K., B. Y. Salazar Vazquez, O. Yalcin, P. C. Johnson, M. Intaglietta, and D. M. Tartakovsky. The effect of small changes in hematocrit on nitric oxide transport in arterioles. *Antioxid. Redox Signal.* 14(2):175–185, 2011.
[47]Sriram, K., A. G. Tsai, P. Cabrales, F. Meng, S. A. Acharya, D. M. Tartakovsky, and M. Intaglietta. PEG-Albumin supra plasma expansion is due to increased vessel wall shear stress induced by blood viscosity shear thinning. *Am. J. Physiol. Heart Circ. Physiol.* 302(12):H2489–H2497, 2012.
[48]Sriram, K., B. Y. Vázquez Salazar, A. G. Tsai, P. Cabrales, M. Intaglietta, and D. M. Tartakovsky. Autoregulation and mechanotransduction control the arteriolar response to small changes in hematocrit. *Am. J. Physiol. Heart Circ. Physiol.* 303(9):H1096–H1106, 2012.
[49]Takahashi, G. H., I. Fatt, and T. K. Goldstick. Oxygen consumption rate of tissue measured by a micropolarographic method. *J. General Physiol.* 50(2):317–335, 1966.
[50]Tangelder, G. J., D. W. Slaaf, A. M. Muijtjens, T. Arts, M. G. Oude Egbrink, and R. S. Reneman. Velocity profiles of blood platelets and red blood cells flowing in arterioles of the rabbit mesentery. *Circ. Res.* 59(5):505–514, 1986.
[51]Taylor, A. E. Capillary fluid filtration. Starling forces and lymph flow. *Circ. Res.* 49:557–575, 1981.
[52]Taylor, G. I. Dispersion of soluble matter in solvent flowing slowly through a tube. *Proc. R. Soc. London A* 219(1137):186–203, 1953.
[53]Torres Filho, I. P., H. Kerger, and M. Intaglietta. pO _2 measurements in arteriolar networks. *Microvas. Res.* 51(2):202–212, 1996.
[54]Tsai, A. G., B. Friesenecker, M. C. Mazzoni, H. Kerger, D. G. Buerk, P. C. Johnson, and M. Intaglietta. Microvascular and tissue oxygen gradients in the rat mesentery. *Proc. Natl. Acad. Sci.* 95(12):6590–6595, 1998.
[55]Winslow, R. M., M. Samaja, N. J. Winslow, L. Rossi-Bernardi, and R. I. Shrager. Simulation of continuous blood O2 equilibrium curve over physiological pH, DPG, and PCO2 range. *J. Appl. Physiol.* 54(2):524–529, 1983.
[56]Womersley, J. R.. Method for the calculation of velocity, rate of flow and viscous drag in arteries when the pressure gradient is known. *J. Physiol.* 127(3):553, 1955.
[57]Zamir, M. The branching structure of arterial trees. *Comments Theor. Biol.* 1:15–37, 1988.
[58]Zimmerman, R. A., G. Severino, and D. M. Tartakovsky. Hydrodynamic dispersion in a tube with diffusive losses through its walls. *J. Fluid Mech.* 837:546–561, 2018.
[59]Zimmerman, R. A., A. Tsai, B. Y. Salazar Vazquez, P. Cabrales, A. Hoffman, J. Meier, A. Shander, D. R. Spahn, J. M. Friedman, D. M. Tartakovsky, and M. Intaglietta. Post-transfusion increase of hematocrit per se does not improve circulatory oxygen delivery due to increased blood viscosity. *Anesth. Analg.* 124(5):1547–1554, 2017.